Basic physics of phototransport as manifested in thin films of In-doped CdTe

I. Balberg,[1] Y. Dover,[1] E. Savir,[1] and P. von Huth[2]
[1]*The Racah Institute of Physics, The Hebrew University, Jerusalem 91904, Israel*
[2]*Department of Materials and Interfaces, The Weizmann Institute of Science, Rehovot 76100, Israel*
(Received 28 April 2010; revised manuscript received 5 October 2010; published 3 November 2010)

Recognizing the interesting effects associated with deep centers in II-VI semiconductors, we reveal the recombination centers map in In-doped CdTe thin films by introducing a systematic and comprehensive phototransport spectroscopy method. The method is more reliable than previous phototransport methods as it is based on a stringent self-consistency of the temperature dependencies of four phototransport properties with a given model. This limits the number of scenarios and narrows the parameter space that can account for the experimental data. We suggest that the deep centers that can account for the data in the studied CdTe system lie both above and below the Fermi level, and that their special distribution can account for some of the "exotic" or "puzzling" phenomena observed in *n*-type CdTe. However, the main purpose of this work is to use the analysis of the In-doped CdTe system as a vehicle for a quantitative comprehensive test of the qualitative physical-analytic ideas of Rose that have guided numerous studies of phototransport in semiconductors. Introducing here the concept of the "center of gravity" of the density of states distribution further extends these basic ideas.

DOI: 10.1103/PhysRevB.82.205302 PACS number(s): 73.61.Ga, 72.20.Jv, 72.40.+w, 71.55.Gs

I. INTRODUCTION

CdTe is a semiconductor that has been investigated intensively in the last fifty years.[1–3] The interest in this material follows from its special properties that make it a convenient arena for the study of new physical phenomena in solids, on the one hand, and a suitable candidate for various photoelectronic applications, on the other hand. As such it became a conspicuous example for the intersection between basic and applied science. In particular, the effect of deep defect states on the microscopic structure and transport has resulted in rich exotic electronic phenomena such that their understanding may be the key for the development of existing and future devices. Notable new phenomena associated with these states are certain photoinduced effects[4] such as photoinduced lattice relaxation[5] and the accompanying persistent photoconductivity in *n*-type, In-doped, CdTe.[6,7] These phenomena add to the conventional widely used photovoltaic-solar-cell applications,[3] optical switching and high density data storage,[8] its potential use as a photorefractive material[9] and photo, x-ray and γ-ray detectors.[10] An important property of CdTe is that it is a bipolar semiconductor, i.e., that both electrons and holes can have sufficiently long lifetimes, and as such, can yield a rich variety of useful homostructures and heterostructures such as the ones that we have demonstrated previously by constructing inverted solar-cell heterostructures.[11] As will be shown below we will make this bipolar property a convenient tool for the study of fundamental properties of this material.

The above-mentioned new photoinduced phenomena in general[12] and for In-doped CdTe, in particular,[13,14] have been explained in terms of metastable deep states associated with a donor (known as the DX) center that involves local lattice relaxations. However, while the deep levels in CdTe control its photoelectronic properties and while numerous studies of these states were and are currently reported we actually know very little about their character in general and their energetic location in particular.[15–18] In view of the limited scope of the present paper we will not review or discuss the many attempts to derive that information and limit our discussion and the cited literature to In-doped CdTe. We should point out, however, that the many data[16,19] that were primarily derived by photoinduced current transient spectroscopy (PICTS) and deep level transient spectroscopy do not yield a consistent picture of where do the defects lie energetically and what are their capture coefficients. For example, numerous values have been assigned to the energy level of the negatively doubly charged Cd vacancy. These range from $E_v+0.05$ eV to $E_v+0.65$ eV, where E_v is the valance-band edge. Similarly for the system of In-doped CdTe that is studied here values from $E_c-0.42$ eV (Ref. 7) to $E_c-0.66$ eV,[20] where E_c is the conduction-band edge, have been attributed to indium defect complexes. In particular, an $E_c-0.42$ eV value was attributed to the DX centers.[7] We will discuss these observations in light of the results obtained in the present study.

An intriguing result of PICTS is the observation in Sn-doped CdTe films[17] that one type of deep centers (at $E_c-0.15$ eV) appears to prevail in the studied temperature range while the concentration of another type of centers of lower energy (at $E_c-0.36$ eV), was concluded to disappear at the lower temperature end of that range. This appears to be an interesting and quite surprising result considering the fact that there is no simple mechanism that can eliminate existing centers just by the variation in temperature.

Following the fact that previous works have concentrated mostly on the spectroscopy of the CdTe system (i.e., only on the determination of the energy levels of the defects[16,19]) and, as far as we know, there were no attempts to derive comprehensive quantitative models of the defect centers that include the capture properties and their distribution throughout the band gap, it appeared to us that such a determination of the defect-state distribution in CdTe systems, in general, and in In-doped CdTe samples, in particular, is called for. This also appears to be a prerequisite for the understanding

of the phototransport properties in general and the "exotic" phenomena (associated with the formation of the DX-like centers[7] or other effects[17]) in it, in particular. Moreover, noting the lack of self-consistency checks between various samples and methods, a method that will have a built-in self-consistency test is needed. In this paper we propose to apply our steady-state phototransport technique[21–25] in order to overcome this difficulty. This spectroscopy is based on the steady-state measurements of four phototransport properties and the application of the stringent condition that the temperature dependencies of all four of them are accounted for by the same states distribution model.[21–25] In this method the experiments are carried out by the use of the photocarrier grating (PCG) technique that takes advantage of the bipolar nature of the photoconductor under study.[23,26] The four phototransport properties considered are the basic mobility-lifetime products[27–30] of the electrons, $(\mu\tau)_e$, and the holes, $(\mu\tau)_h$, as well as their well-known corresponding light intensity exponents,[28–30] γ_e and γ_h. The experimentally obtained temperature dependencies of these properties are compared then with results that are obtained in computer simulated models. This is done by a careful systematic increase in the complexity of the model until there is a model for which all four dependencies of the model simulations match the experimental results. The simplest model is in which the defects have the same energy level with a minimum number of corresponding parameters. The complexity of a model is increased by increasing the number of parameters or their temperature dependence. If this appears to be insufficient we turn to a system of a higher number of levels and continue as above. We have confirmed already in other systems that the above requirement regarding the results of all four phototransport properties is stringent enough to limit considerably the possible scenarios that can account for the experimental data.[22,23] We also note in passing that in the present context utilizing the bipolar nature of CdTe, that enables the study of the properties of the minority carriers simultaneously with those of the majority carriers, provides an advantage over the transient methods that are based only on the majority carries. This is since the latter are myopic to the states that control the recombination kinetics of the minority carriers.

Turning to the interesting system of In-doped CdTe that we studied here we noted that we have to apply samples that have a high enough In content in order to yield detectable In complexes that yield DX centers. On the other hand, the content has to be low enough to avoid persistent photoconductivity[4] that may jeopardize the simple derivation of the above four quantities from the experimental data. This condition appears to be satisfied in our samples that have a concentration of 10^{18} cm^{-3} In atoms. We note then that the energetic position and the parameters of the defect centers that we derive here are associated with such samples.

Last but not least is the basic physics insight that is gained by the comparison of simulated results with the experimental data. In particular, the effect of the various parameters associated with the recombination process is evaluated quantitatively. This enables an extension of the original ideas of Rose[28] that have guided the research in the field in the last 50 years. In particular, the effect of the position of the Fermi level, E_F, on the phototransport properties, that was shown by Rose to be the key to the understanding of the behavior of γ_e and γ_h, is evaluated here quantitatively. The importance of these parameters is that unlike the $\mu\tau$ products they are associated solely with the recombination kinetics. In addition, we found that by considering our results we are able to resolve the intriguing behavior observed in Sn-doped CdTe (Ref. 17) without assuming the "disappearance" of deep defect states in that system.

The structure of the paper is as follows. In Sec. II we describe the sample preparation and the experimental method for the derivation of the phototransport properties. This is done very briefly since these were described in detail previously.[11,23,26] Then, in Sec. III, we present an outline of the numerical-simulation method applied in the present work. Because of the central role of these simulations in the evaluation of the state distribution in the system under study we present more of their details in Appendices A and B. In Sec. IV we present the phototransport data and in Sec. V we provide the main results of our systematic computer simulations study. There, we tried to reproduce the experimental results by systematically constructing possible model scenarios. A discussion of the results and their comparison with previous data as well as the corresponding more general consequences of this study are given in Sec. VI.

II. EXPERIMENTAL DETAILS

Our polycrystalline CdTe films have been deposited on both *p*-type diamond and Corning 1737 glass substrates using CdTe/In sublimation/evaporation sources. The thickness of the studied films was on the order of 10 μm and the typical CdTe grain size in them (as determined by our atomic force microscopy images) was on the order of 0.4 μm. Secondary ion mass spectroscopy profiling has indicated a concentration of 10^{18} cm^{-3} In atoms in the films, and analysis of capacitance-voltage measurements indicated uncompensated donor charges with a concentration of 10^{14} cm^{-3}. In particular, by applying x-ray photoelectron spectroscopy (XPS) we found that the Fermi level in our samples lies at 0.31 eV below the conduction-band edge. Since our phototransport results were much the same for the films on either substrate we will show here only the results obtained on a sample deposited on the glass substrate since for these samples the nonparticipation of the substrate in the transport and phototransport is secured. The films' deposition procedure and their structural and photovoltaic properties as well as their *n*-type character were described in detail elsewhere[11] and will not be repeated here. For the electrical measurements silver contacts 0.4 mm apart were evaporated on top of the films.

The experimental method for the derivation of the phototransport properties have been reviewed in detail in text books and in our previous works. In particular, our measurements of the mobility-lifetime $(\mu\tau)$ products and the light intensity exponents γ_e and γ_h of the electrons and holes have been described previously.[21–26] Briefly, this method is based on the measurements of the photoconductivity, σ_{ph}, and the ambipolar diffusion length, L, in the PCG configuration in

the 80–300 K temperature range. The illumination of the sample was provided by a He-Ne laser with a power of 15 mW. From the values of these quantities we derive then the mobility-lifetime product of the majority carriers (the electrons in the present *n*-type material) by applying the relations $(\mu\tau)_e=\sigma_{ph}/Gq$ for the electrons and $(\mu\tau)_h=qL^2/2kT$ for the holes. Here, q is the electronic charge, kT is the thermal energy, and G is the carrier generation rate. The maximum value of G in our experimental setup was 10^{21} cm^{-3} s^{-1}. Assuming[28,29] the conventional power-law dependence of the $\mu\tau$ products on G, we obtained from the measurements the corresponding light intensity exponents using the relations $\gamma_e-1=d[\log_{10}(\mu\tau)_e]/d[\log_{10} G]$ and $\gamma_h-1=d[\log_{10}(\mu\tau)_h]/d[\log_{10} G]$ over the $10^{19}\leq G\leq 10^{21}$ cm^{-3} s^{-1} range. It is quite important to note in passing that γ_e and γ_h are differentially sensitive quantities for the determination of the energy distribution of the levels associated with the recombination centers in the forbidden gap of a photoconductor (see below).[28–30]

III. MODELS, PARAMETERS, AND SIMULATIONS

Once the four experimental temperature dependencies of the mobility lifetime products and the light intensity exponents were available we have turned to the simulations in an attempt to try and fit model-simulation results to the experimental data. The present polycrystalline CdTe system is an ideal case for trying to account for the experimental data by starting from the simplest possible model of recombination, i.e., the Shockley-Read model.[27,29] This is because this system may have, in principle, centers with a few discrete levels and/or a continuous distribution of levels due to the possible variation in the environment of a dopant's complex and/or the disorder associated with interfaces (grain boundaries) between the crystallites.[3,11] We started our simulations then with models of defect-center states that have a single energy level. When this was found to be insufficient we turned to plausible temperature-dependent parameters within the framework of this single-level model. When the latter step turned to be insufficient we proceeded to models of two types of centers where each type has a different energy level. The model and the equations that we have used are those of Shockley and Read[27] for one type of centers while for more than one type of centers we have applied models of others[29] and ours.[23] Since all the equations that describe models of discrete defect states[29] and the model that considers also a continuous distribution of states[21] are well known, they are given (in Appendix A) here only in a concise form. In all our discussions we consider only the "small signal" case where one assumes that the concentration of the "free" charge carriers is considerably smaller than the concentration of defect centers.

In our simulations the parameters adopted were either derived by us experimentally (e.g., the position of the Fermi level, E_F, see below) or taken from other known data (e.g., values of the carrier mobility and capture coefficients as estimated from previous reports[20]). In Table I we list the parameters that were taken to be constants in the simulations as well as the parameters that were varied. For the latter we present in the table their more common values.

TABLE I. List of the commonly used parameters in our simulations.

$E_v=0$, $E_c=1.6$ eV
$N_{co}=N_{vo}=2.5\times10^{19}$ cm^{-3}
$G=10^{19}$ cm^{-3} s^{-1}.
$E_F=1.34$ eV, $E_t=1.35$ eV, $E_{t1}=1.2$ eV, $E_{t2}=1.4$ eV
$N_t=N_{t1}=N_{t2}=10^{17}$ cm^{-3}
$C_n=C_{n1}=C_{n2}=C_p=C_{p1}=C_{p2}=10^{-8}$ cm^3 s^{-1}
$\mu_e=10^3$ cm^2/V s or $10^3(300/T)^{1/2}$ cm^2/V s, $\mu_h=10$ cm^2/V s
$N_{tG}=10^{15}$ cm^{-3} eV^{-1}, $E_{tG}=1.14$ eV, $W=0.05$ eV

An important parameter that can tell us about the system under study is the position of the Fermi energy, E_F, which is also the key to the understanding of the kinetics of the system as was analyzed by Rose.[28] This quantity can be derived from the temperature dependence of the dark conductivity, $\sigma=\sigma_o\exp(-E_a/kT)$, where σ_o is the conductivity prefactor and E_a is the activation energy, as follows. The behavior shown in Fig. 1 for the sample under study indicates a variation in E_a from about 0.15 eV at 180 K to 0.26 eV at 300 K. We further note in passing that room-temperature activation energies such as found here have been previously observed in In-doped CdTe films by others.[7] This behavior is not typical to the extrinsic range of a semiconductor where the carrier concentration is fixed. On the other hand, the values of the activation energy involved and the increase in E_a with temperature may indicate the transition from an extrinsic to an intrinsic regime in a semiconductor.[31] In particular, this interpretation would suggest that states that lie below the Fermi energy, E_F, contribute to the electron concentration in the conduction band. In principle these may be the valence-band states or localized band-gap states.[32–34] Hence, the simplest way to interpret the value of E_a at room temperature (the highest temperature that we use in the present study) is that it is the lowest bound of E_c-E_F in our samples. In other words, we can conclude that our E_F lies below $E_c-0.26$ eV. This conclusion is well supported by our XPS value that was mentioned in Sec. II. Considering that the band gap of CdTe is about 1.6 eV (Refs. 3 and 35) we choose

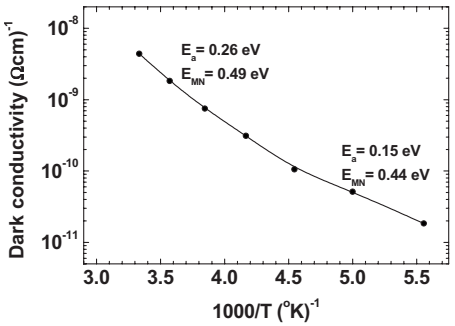

FIG. 1. The temperature dependence of the dark conductivity in the sample on which the phototransport data were obtained. The activation energy E_a and the possible continuous-states $E_{MN}=E_c-E_F$ values, in the lower and upper temperature regimes, are indicated.

for our initial standard, a temperature-independent E_F level that is located at $E_c-0.26$ eV$\equiv E_v+1.34$ eV, throughout the temperature range under study.

While the above applies to the case of discrete levels in the band gap, if we assume a continuous distribution of states, as in amorphous semiconductors, we have to consider the "statistical shift" and take σ_o to have the "minimal metallic conductivity" value of $\sigma_o=150$ $(\Omega\ \mathrm{cm})^{-1}$.[32–34] Applying this consideration to the results of Fig. 1 yields that the conductivity activation energy, $E_{MN}(=E_c-E_F)$ is 0.49 eV at the high-temperature end, and 0.44 eV at the low-temperature end. In that case E_c-E_F is roughly a constant and we can proceed by considering it as such. In particular, since the band gap is 1.6 eV (Refs. 3, 35, and 36) we have also considered the value of $E_c-E_F=E_c-0.44\equiv E_v+1.16$ eV and intermediate cases, between this value and the above $E_c-E_F=0.26$ eV value.

The other known parameter from our own experimental work is the range of the applied photogeneration of the carriers, G, which we have varied between 10^{19} and 10^{21} $\mathrm{cm}^{-3}\ \mathrm{s}^{-1}$. In our comprehensive simulation study, apart from E_F and G we have varied all other parameters involved in the recombination process in order to evaluate their effect on the qualitative and quantitative behaviors of the four phototransport properties.

For other parameters of the system we turned to the literature. For the mobility values μ_e and μ_h we found that they are usually given to be on the order of 10^2-10^3 $\mathrm{cm}^2/\mathrm{V\ s}$ for the electrons[1,15,36] and on the order of 10 $\mathrm{cm}^2/\mathrm{V\ s}$ for the holes.[15,36] For our purpose it will be important to note that, as in similar II-VI compounds, μ_e decreases with temperature while μ_h is almost temperature independent in the temperature range that we study in this work. The mentioned decrease with temperature is due to phonon scattering but in practice, due to the thermally activated impurity scattering, the decrease with temperature is weaker than expected from the former process.[37]

The other important parameters are the capture coefficients of the two carriers. Since a very wide range (between 10^{-6} and 10^{-10} $\mathrm{cm}^3\ \mathrm{s}^{-1}$) of values of these parameters has been reported in the literature[8,20] we took reasonable intermediate values at our starting point and then varied them over a wide range in order to get the best agreement with the experimental data. The initial fixed four values of the capture coefficients and typical initial values of the other parameters used in the present work are listed, following their definition in Appendix A, in Table I. Variations from the values given in that list will be detailed as we go along with the presentation of our simulations.

Let us stress that of our comprehensive simulation study we will present, for brevity, mainly the results that resemble closely the experimental data, while the many other scenarios that we studied and that did not yield agreement with the experimental data, will be mentioned only briefly. In our numerical simulations we have first chosen the model, i.e., the set of equations that describes the recombination level structure, as given in Appendix A, following Refs. 23 and 29. Then, in order to fit the experimental data, we varied first the parameters that we expected to "improve" the quality of the fitting. When the variations were exhausted we have varied the previous-unvaried parameters to find whether an improvement is achieved. This was repeated until we concluded that for a given model no further improvement could be obtained. In solving the equations (as given in Appendix A) we derived the steady-state concentrations of the "free" electrons, n, the "free" holes, p, as well as the concentration of captured electrons, n_t, in each of the assumed levels. For the comparison with the experimental phototransport data the calculated values of n and p were expressed as usual[21–30] in terms of $(\mu\tau)_e=\mu_e(n-n_0)/G$ and $(\mu\tau)_h=\mu_h(p-p_0)/G$, where n_0 and p_0 are the electron and hole concentrations in the dark. The numerical procedure used in this study is described in Appendix B.

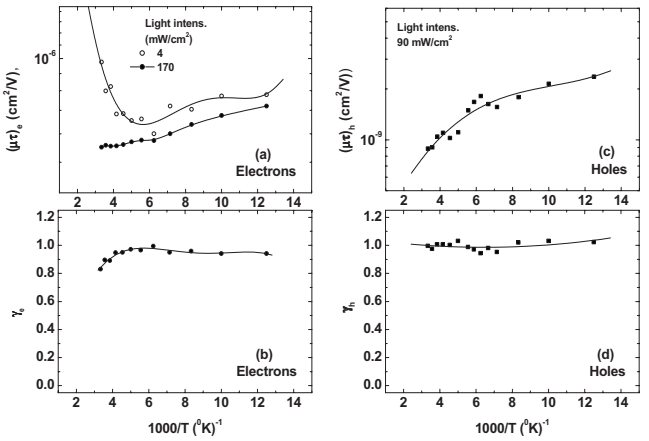

FIG. 2. The temperature dependence of the four phototransport properties in our In-doped CdTe films. In Fig. 2(a) we show the $(\mu\tau)_e$ results for the two extreme illumination intensities (carrier generation rates) that were used.

IV. EXPERIMENTAL RESULTS OF THE PHOTOTRANSPORT

Following the above brief reviews of our experimental and computational procedures, let us turn to the phototransport results that we obtained. These data were found to be much the same for the various films that we mentioned in Sec. II, independent of the substrates on which they were deposited. Correspondingly, we show here the results for the sample that was deposited on the Corning 1737 glass. We will also give here a short qualitative-phenomenological explanation of these results.

The temperature dependencies of the four phototransport parameters that we measured are shown in Fig. 2. Starting with the electrons we see in Fig. 2(a) that for the high illumination intensities, as the temperature increases, there is a monotonic decrease of $(\mu\tau)_e$. This is in contrast with the increase in $(\mu\tau)_e$ at the higher temperatures that we found at the lower illumination intensity. Typically in photoconductors[29] there is a monotonic increase in the carriers lifetime with temperature due to the corresponding decrease in the effective concentration of recombination centers (as to be expected from the narrowing of the energy separation of the two demarcation levels[28,29]). In principle, a decrease in the $(\mu\tau)_e$ product as obtained here may be a

result of the change in the type of centers that participate in the recombination process (as in thermal quenching phenomena[21,28,29]) and/or due to the dominating temperature dependence of the mobility (see below). Still, the unusual behavior exhibited by the temperature dependencies of $(\mu\tau)_e$ in Fig. 2(a) yields one of the difficulties in a straight-forward interpretation of the data. However, as shown in Sec. V, it also suggests a clue for the spectroscopic analysis of the results.

In Fig. 1(b) we see that γ_e has practically the value of unity up to 200 K and then it decreases to about 0.8. While *a priori* there may be quite a few speculations as to the qualitative explanations of this behavior, only a more specific model can account for it quantitatively. In passing we note that the best known model that accounts for such a behavior is the change in the width of the conduction-band tail in disordered semiconductors.[28,29] In fact, as we will see in Sec. V, this is not the model that emerges in the present system. On the other hand, the consideration of this variation in γ_e will be very helpful in fine tuning the model that accounts for all the observed phototransport properties.

Turning to the behavior of the holes we see that the decrease in $(\mu\tau)_h$ (i.e., here the mobility-lifetime product of the minority carriers) with temperature in Fig. 2(c) is similar, for the entire range of the illumination intensity that we used, to that of the majority carriers under the high illumination intensity. Following the fact that the well-known behavior of the demarcation levels[28] cannot yield a simultaneous decrease in both τ_e and τ_h with the increase in temperature, and the hinted increase in τ_e for the low illumination intensity in Fig. 2(a), we can tentatively assume that the temperature dependence of the $(\mu\tau)_e$ is dominated by the temperature dependence of μ_e while the temperature dependence of $(\mu\tau)_h$ is dominated by the temperature dependence of τ_h. This assumption, will be well justified in Sec. V. Finally, as shown in Fig. 2(d), γ_h can be considered to be unity throughout the entire temperature range under study. Such a behavior indicates that the effective concentration of recombination centers that are available for the holes is essentially independent of the changes in the concentration of the carriers that are induced by the optical excitation.

Before turning to the simulations let us underline then that the salient features of the experimental data that have to be reproduced by the computer simulations are the decrease in γ_e from about 1 to about 0.8, the constant $\gamma_h=1$ value, and the decrease in $(\mu\tau)_h$ with temperature.

V. RESULTS OF THE COMPUTER SIMULATIONS

Turning to find the simplest model that may account for the experimental data we consider first the model of a single-level group of defect centers in a semiconductor with a temperature independent value of E_F [i.e., Eqs. (A1)–(A3) with $i=1$]. For E_F we choose that $E_F=E_c-0.26$ eV (see Sec. III). We note, however, that even this simplest Shockley-Read model[27] has already very many parameters to yield numerous behaviors of the phototransport properties in general and of the photoconductivity, σ_{ph}, in particular (see also Sec. VI). It is then *only the stringent condition of our method* (i.e., the requirement to fit the simulation results to *all* four phototransport properties) that is expected to narrow down considerably the volume of the parameter space.[23] While the most natural explanation of the decrease in $(\mu\tau)_e$ with temperature in CdTe is the decrease in $\mu_e(T)$ we started, for simplicity, with the assumption of constant μ_e and μ_h values and examined critically whether the experimental results can be accounted for solely by a lifetime effect which depends only on the concentration (N_t) and properties (energy location, E_t, and capture coefficients C_n and C_p) of the recombination centers. Before we turn to the simulations, and for providing a common ground for the discussion of the results, we reserve in what follows the conventional term of a "majority carrier" to the carrier for which its $\mu\tau$ product is larger, as this is the quantity that is measured by the conventional photoconductivity. The other carrier, i.e., the one that determines the ambipolar diffusion length, is the one with the smaller $\mu\tau$ to which we refer as the minority carrier. We distinguish then between the situation where the material is an *n*-type photoconductor (more photoelectrons than photoholes, i.e., $n>p$ or $\tau_e>\tau_h$) and the situation where the electron is the majority carrier $[(\mu\tau)_e>(\mu\tau)_h]$. One notes then that the majority carries in a *p*-type photoconductor may be the electron in the case where its mobility is large enough to offset the larger lifetime of the hole.

Below we consider then the single-level centers for the three scenarios; $E_t\approx E_F$, $E_t<E_F$, and $E_t>E_F$, and then we will turn to the two levels scenario. Finally, we will consider the scenario of a continuous distribution of states.

A. Single level with the $E_t\approx E_F$ scenario

In order to gain a better understanding of the basic physics of the recombination processes that are involved and in order to account for the experimental observations, shown in Fig. 2, we start by the simplest model in which we even ignore the experimentally observed temperature variation in γ_e (the decrease in γ_e toward 0.8 above 200 K). The $\gamma_e=\gamma_h=1$ scenario has been discussed in the literature[28–30] for the small signal ($n,p\ll N_t$) case and for the case where the energy level of the recombination centers coincides (or almost coincides) with E_F, when both are well removed from the band edges so that the thermal excitation of the carriers to the bands can be considered negligible. In that scenario the defect-centers' occupation is not effected significantly by the concentration of the excited carriers and simple analytic considerations apply.[28,30] Correspondingly, the carriers lifetime is not sensitive to the carrier generation rate G, and $\gamma_e=\gamma_h=1$.

In order to appreciate the temperature dependence of the mobility-lifetime product under this simple scenario that was discussed first by Rose[28] and later by one of us[30] within the framework of the relative positions of E_t and E_F, we run here [using Eqs. (A1)–(A3)] a case for E_t that lies just above E_F, i.e., for $E_t-E_v=1.35$ eV. The concentration of recombination centers was taken to be $N_t=10^{17}$ cm^{-3} and they were assumed to have a neutral character, i.e., the capture coefficient of the electrons, C_n, and the capture coefficient of the holes, C_p, were taken to be equal. As a reasonable value (see

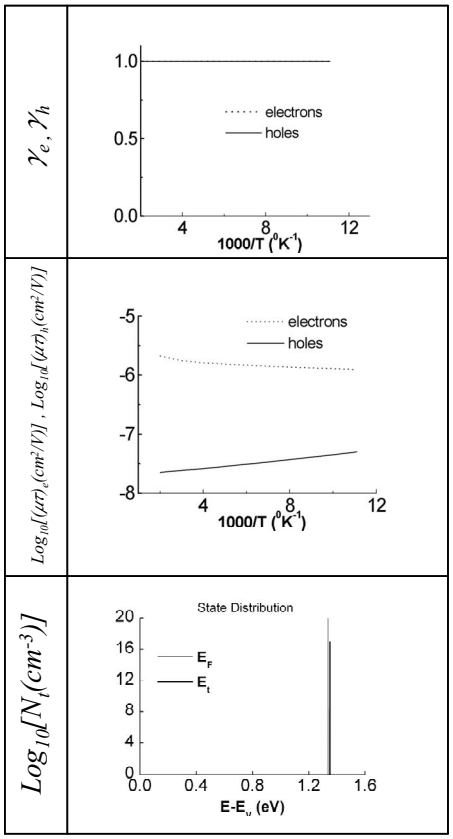

FIG. 3. The simulated temperature dependence of the four phototransport properties and the energy level of the defect center in the simulated one-level model. The height of the line at E_t conveys the concentration of the centers. Also indicated is the position of the Fermi level. The parameters used in this simulation are given in Table I.

Sec. III) we assume then that $C_n = C_p = 10^{-8}$ cm^3 s^{-1}. In order to separate the $\mu\tau$ products of the two carriers, we use tentatively different values for the mobilities, $\mu_e = 10^3$ cm^2/V s and $\mu_h = 10$ cm^2/V s. These values are born out by values given in the literature for CdTe crystals.[1] The result of the simulation for the four phototransport properties as well as the assumed positions of the Fermi energy E_F and the center's level E_t are shown in Fig. 3. The "height" of the segment at E_t denotes the value of N_t. The proximity of E_t to E_F yields the overlap of γ_e and γ_h at the value of unity while the computed behavior of the $\mu\tau$'s can be understood as follows. Since $E_t > E_F$, the higher the temperature the larger the concentration of electron occupied centers at of E_t and thus the lower the concentration of hole occupied centers, $p_t = N_t - n_t$ (that are available for electron recombination). This yields of course the increase in the electron's lifetime, τ_e, and the decrease in the holes lifetime, τ_h, with temperature. We note that since at E_F, $p_t \approx n_t$ and since we assumed that $C_n = C_p$ we got here that the ratio of the two $\mu\tau$ products is quite close to the ratio of their mobilities (10^2). As expected we found that the feature of the decrease in $(\mu\tau)_h$ with temperature for $E_t > E_F$ is quite general regardless of the other recombination parameters (e.g., the values of the capture coefficients).

In our simulations we considered the limits of the $\gamma_e = \gamma_h = 1$ behavior as the energetic interval $E_t - E_F$ is varied. For example,[28,30] if E_t lies far below E_F the charge neutrality condition $p_t - p_{to} = n - n_o$ (where p_{t0}, n_{t0}, and n_0 are the values of p_t, n_t, and n at equilibrium) will yield that $\tau_e \sim 1/(n - n_o)$ and thus $\gamma_e = 1/2$. Similarly, for E_t that lies far above E_F, we expect that $\tau_h \sim 1/(p - p_o)$ and thus that $\gamma_h = 1/2$. To find the interval for which the $\gamma_e = \gamma_h = 1$ result is maintained we considered various E_t values establishing that the $\gamma_e = \gamma_h = 1$ result under the above C_n, C_p, and N_t values is maintained for the energy interval $E_t = E_F \pm 0.05$ eV. The importance of this observation is that it puts the *missing quantitative limits* on the qualitative scenario expected from the simple theory of Rose.[28] As to be expected from the $\gamma_h = \gamma_h = 1$ result all the quantities that we study and shown here in Fig. 3 are found to be independent of G for the G range, $10^{21} \geq G \geq 10^{15}$ cm^{-3} s^{-1}, that is used in our simulation work and is typical for phototransport studies in semiconductors.

Considering the behavior of the $\mu\tau$ products within the $\gamma_e = \gamma_h = 1$ scenario, i.e., the fixed E_F and E_t such that $E_t - E_F$ is relatively small, we would expect that the τ_e and τ_h, and thus the n and p, values will simply scale with the values of C_n and C_p and thus, for donor like ($C_n > C_p$) states, we expected and found that the $(\mu\tau)_e(T)$ and $(\mu\tau)_h(T)$ curves shown in Fig. 3 (when a temperature-independent mobility was assumed) intersect at some temperature, indicating the n-type to p-type transition.

We noted in Sec. II that in CdTe (Refs. 1, 15, and 36) and similar materials[37] there is a decrease in the electron mobility with temperature in the temperature range under study while the hole mobility in CdTe was reported[15,38] to be quite temperature independent there. For example, noting that the room-temperature values of the electron mobility in single crystals of CdTe are between $\mu_e = 10^2$ and 10^3 cm^2/V s, and that the hole mobility is around 10 cm^2/V s,[1] we considered the phenomenological dependence of $\mu_e = 10^3(300/T)^{1/2}$ cm^2/V s together with a constant, $\mu_h = 10$ cm^2/V s, value. Indeed, for these μ_e and μ_h, we found an excellent agreement with the corresponding temperature dependence of the electron [lower curve in Fig. 2(a)] and hole $\mu\tau$ products of Fig. 2. These results are quite robust for our single-level model as they were found to be maintained for a constant, $N_t C_n = N_t C_p = 10^9$ s^{-1} value. As we will see throughout this work and as was pointed out above *we could not find any other scenario (of those considered in this work, i.e., the simplest possible scenarios) that can account for all the three other experimental behaviors of the phototransport properties without assuming a decrease in μ_e with temperature*. The fact that this decrease in μ_e with temperature is well known for CdTe (Refs. 1 and 37) gives us then confidence that the approach that we use in our simulations is reliable. In passing we note of course that, since, say; $(\mu\tau)_e$ is also proportional to the $\mu_e / C_n N_t$ product, one cannot distinguish *a priori* the influence of each of the three parameters. However, having some prior knowledge on each of them, as in the present study, enables a more detailed "effective" model in general, and the attribution of the temperature dependence of the $\mu_e / C_n N_t$ product to one or more of these parameters, in particular.

In trying to evaluate the behavior shown in Fig. 2, still within the single-level model, we have to consider the pos-

sible effect of temperature on the capture coefficients. Obviously, to account for the decrease in both τ_e and τ_h with temperature we would need to introduce an increase in the capture coefficients with temperature. While not unreasonable (and since the centers can be activated under some conditions[39]) this is quite opposite to the usually observed and expected (carrier activated) behavior.[28] However, since such an increase in C_n and/or C_p with temperature can be a result of quite a few scenarios[39] (e.g., the increased trapping by DX centers) we did consider this case in some detail. Indeed, we were able to reproduce the decrease in $(\mu\tau)_e$ with temperature by a phenomenological behavior such as $C_n = 10^{-8}(T/300)^2$ cm^3 s^{-1}. However, since we do not have an *a priori* knowledge or another justification for such temperature dependence of the capture coefficients, we prefer, at present, the above scenario of the mobility decrease with temperature for which there is evidence in the above cited literature. Of course, the other possible temperature-dependent parameter in the present simple, one energy level, model may be the position of E_t with respect to E_F. This position variation will be considered in the following section.

B. Single level with a $\gamma_e \neq 1$ and/or a $\gamma_h \neq 1$ scenario

As we have pointed out above the $\gamma_e = \gamma_h = 1$ case is a very good starting point for the introduction of the system with a single-level defect centers. It is, of course, unsatisfactory when we consider the decrease in γ_e from 1 to 0.8 between 200 and 300 K in Fig. 2(b) and the different behaviors of $(\mu\tau)_e$ for the low-G and the high-G cases that were shown in Fig. 2(a). We tried then first to reproduce the entire experimental behavior shown in Fig. 2 by having an E_t that is well (a few kT) separated from E_F. This is since we know[28,30] that under small signal conditions $(n,p \ll N_t)$, as in our work, a $\gamma_e \neq 1$ behavior can be obtained only when E_t is removed from E_F.

Starting with the $E_t < E_F$ scenario we recall that in this case[28,30] the charge neutrality is conserved by a balance between the concentration of the free majority carriers (in our case the electrons), n, and the hole occupation of the recombination levels, p_t, when the levels are almost fully occupied by electrons. This yields then $\gamma_e = 1/2$ and $\gamma_h = 1$ values for the entire temperature range except for the very high-temperature range where the concentration of the thermally excited electrons, n_0, exceeds p_t. For our purpose, of trying to simulate the behavior shown in Fig. 2, the important observation is that the increase in γ_e with temperature, from 1/2 to 1, is in sharp contrast with the experimentally found decrease in γ_e from 1 to 0.8 over the same temperature range. Following that we turned to the other possible scenario, i.e., where E_t is well removed from E_F but $E_t > E_F$. In that case the material is n type in the dark while under illumination it can become a p-type photoconductor. To follow this more complicated case we started, for simplicity, with the deeper possible E_F value (see Sec. III) by taking $E_c - E_F$ at 0.44 eV, so that the material, in the dark, is a "weak" n-type semiconductor. Indeed considering this case with $E_t - E_F = 0.24$ eV we got, as shown in Fig. 4, the expected behavior. At low temperatures the material is a p-type photoconductor, $\gamma_h = 1/2$, and $(\mu\tau)_h$ is practically a constant. The $\gamma_h = 1/2$ comes of course from the charge neutrality conditions [i.e., the equality of n_t and p (Ref. 28)]. On the other hand, there are less photoelectrons than photoholes, and thus, $\gamma_e = 1$, and $(\mu\tau)_e$ is a constant. As the temperature increases there is an increasing concentration of the thermally excited electrons, n_o, yielding the increase in the electron occupation of the centers and thus the simultaneous increase in the electron lifetime with the decrease in the hole lifetime. When n_o dominates the recombination, both γ's tend to unity. If however E_F is higher (the n-type character of the material in the dark is enhanced) the transition due to the thermal excitation starts to dominate the system at lower temperatures. For our purpose of evaluating the experimental behavior, the important point here is that the $E_t > E_F$ case provides the key characteristic of the behavior shown in Fig. 2(b), i.e., the decrease in γ_e from unity upon the increase in temperature.

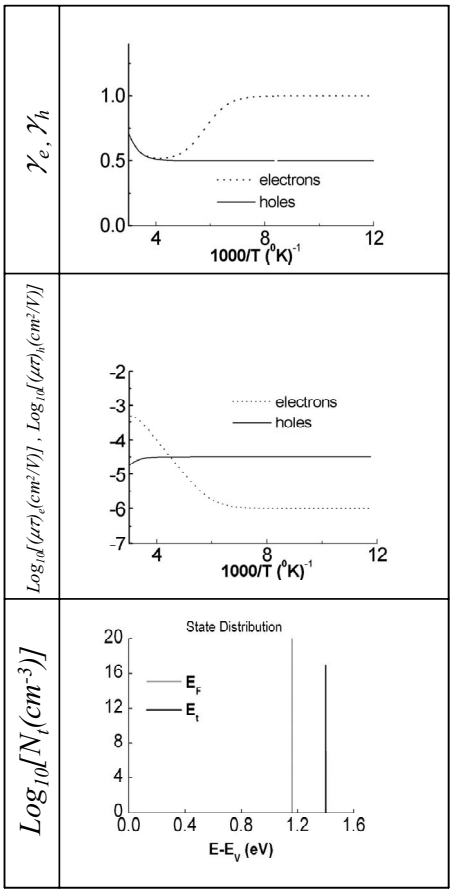

FIG. 4. The simulated temperature dependence of the four phototransport properties and the corresponding energy levels in the system. This is for a defect-center level $(E_t - E_v = 1.4$ eV) that is well removed from a deeper $(E_F - E_v = 1.16$ eV) Fermi level. The other parameters are as in Table I.

Following however the need to reproduce the decrease in γ_e with temperature, as well as the constant $\gamma_h = 1$ value, that we found experimentally, and our knowledge[30] that these values depend on the $E_t - E_F$ separation, we have tested an empirical temperature-dependent separation of $E_t - E_F$ such that at low temperature $E_t(T)$ will yield the $\gamma_e = \gamma_h = 1$ behavior (i.e., E_t just above E_F) and at high temperature E_t will

yield a γ_e value that is smaller than unity while keeping the $\gamma_h=1$ value (i.e., E_t is shifted to below E_F). In principle, of course, this may be due to an E_F that simply increases with respect to E_t or due to the decrease in E_t with increasing T. The first possibility is however in contrast with the behavior shown in Fig. 1 (E_c-E_F should decrease rather than increase then) and with the expectations for conventional semiconductors.[31] Hence, if any, the latter scenario is much more likely. Correspondingly, we checked then the possibility of the decrease in E_t with temperature. In the choice of parameters for that case we were guided by the two-level scenario that will be introduced below. In particular, we searched for phenomenological dependencies of $E_t(T)$ that could reproduce the experimental results. Such dependencies were $E_t=E_v+1.35$ eV for, say, $T<80$ K and $E_t=E_v+1.35-0.15(T/350)^2$ eV, or $E_t=E_v+1.35-0.15(T/325)^3$ eV, for higher temperatures. These shifts of E_t are on the order of the changes in the band gap in this material.[1] At this stage the important point is that using these dependencies we did indeed reproduce the experimentally observed γ_e, γ_h, and $(\mu\tau)_h$ behaviors and, if the above suggested temperature dependence of μ_e is introduced, also the $(\mu\tau)_e$ behavior. We note however that we do not have an *a priori* justification or physical grounds for such a shift of E_t except that the behavior of this model resembles effectively the two-level scenario of Sec. V C.

C. Two-level scenario

We start our consideration of the next set of possible scenarios with temperature-independent recombination parameters but with the inclusion of two types of centers with two different energy levels: the first level, E_{t1}, lies below E_F in order to provide the sublinear γ_e values at the higher temperatures and a second level, E_{t2}, lies just above E_F, in order to secure the low-temperature $\gamma_e=1$ result. This is since if both levels lie on the "same" side of E_F we get essentially an effective single-level scenario such as the one considered above. Our expectation is then that the two-center model with levels on the "opposite" sides of E_F will yield the behavior of γ_e, γ_h, and $(\mu\tau)_h$ as in Fig. 2. As with the single-level model we could not reproduce in our many trials the observed decrease in $(\mu\tau)_e$ with temperature [Fig. 2(a)] when a temperature-independent μ_e value was assumed. Following these expectations we constructed a two-level model with $E_F-E_v=1.34$ eV, $E_{t1}-E_v=1.20$ eV, and $E_{t2}-E_v=1.35$ eV and took μ_e to be $10^3(300/T)^{0.6}$ cm^2/V s, noting that this behavior represents well a mobility that is determined by both, phonon and impurity scattering processes.[37] Indeed, the basic qualitative features of the experimentally observed behavior in Fig. 2 were confirmed.

Following this qualitative agreement we tried then to narrow down the parameter space in order to approach the experimental results of Fig. 2 more quantitatively. An important feature was that with decreasing G (in our experimental range of $10^{19}\le G\le 10^{21}$ cm^{-3} s^{-1}) the onset of the decrease in γ_e shifts to lower temperatures. This behavior is a clear indication that the E_{t1} level becomes more involved in the recombination as the temperature increases. In other words, the increase in temperature provides enough hole occupied recombination sites at E_{t1} so that this channel of recombination determines the electrons lifetime. This is quite a significant indication that *our two-level model captures the essentials of the behavior shown in Fig. 2*.

Varying the values of the capture coefficients and the concentration of the two types of defects, for a given two-level scenario (when $E_{t2}>E_F>E_{t1}$), we found that the simulated behavior is not too sensitive to the ratio of the values of the capture coefficients of the two charge carriers. However, the centers of the upper level (E_{t2}) cannot be acceptorlike and the centers of the lower level (E_{t1}) cannot be donorlike. Of course, since the behavior of the two levels is interdependent we cannot suggest well-defined values for the capture coefficients of either level. Considering the need for a quantitative fit and from the findings of the ranges of values of N_{t1} and N_{t2} (for which we found the transition in the recombination channel) we could conclude that the capture coefficients of the two levels are on the order of 10^{-9} cm^3 s^{-1} and that they can be in the range of $10^{-11}-10^{-7}$ cm^3 s^{-1}. On the other hand, our method enables the derivation of relatively narrow ranges for the concentrations of the recombination centers, around $N_{t1}\approx 10^{15}$ cm^{-3} and $N_{t2}\approx 10^{17}$ cm^{-3}, for the above rather wide range of their capture coefficients. To make sure that the above behavior is due to two levels and cannot be reproduced by a single level we checked the above model with alternatively, diminishing, each kind of centers, finding indeed the behavior of the expected corresponding single level. The latter results show clearly that the resemblance we got to the experimental data is due to *a combination of the recombination in two types of centers.*

In our simulations we found an increase in γ_e at the highest studied temperatures. This behavior, as well as the behavior of the mobility-lifetime products there, was shown to be determined by the thermal generation of the free carriers. We did not see such a behavior in the experimental results. This suggests that the true position of E_F is lower than assumed in our model, so that the role of these thermally excited carriers, which is not important for our spectroscopy, should not be taken into account. The lower E_F is in agreement with our evaluation, in Secs. II and III, that the possible maximum value of E_c-E_F can be as large as 0.44 eV. This suggests that the E_c-E_F value should be an intermediate one between 0.26 and 0.44 eV. Following these considerations and after a detailed study of the effect of the position of E_{t1} and E_{t2} on the results we have checked the effect of the position of E_F on the results while keeping the intervals $E_{t2}-E_F=0.01$ eV and $E_F-E_{t1}=0.19$ eV constant. We carried out the simulation then for $E_F=E_v+1.20$ eV and $E_F=E_v+1.28$ eV. The results shown in Fig. 5 for the latter case are *the closest to the experimental data that we ever got*, supporting our conjecture that the value of E_c-E_F in our experimental results is, as suggested above, somewhat larger than 0.26 eV.

D. A Gaussian distribution of states

We have seen above that a single discrete-level state can reproduce the experimentally observed features only if we let the defect level shift with temperature from above to below

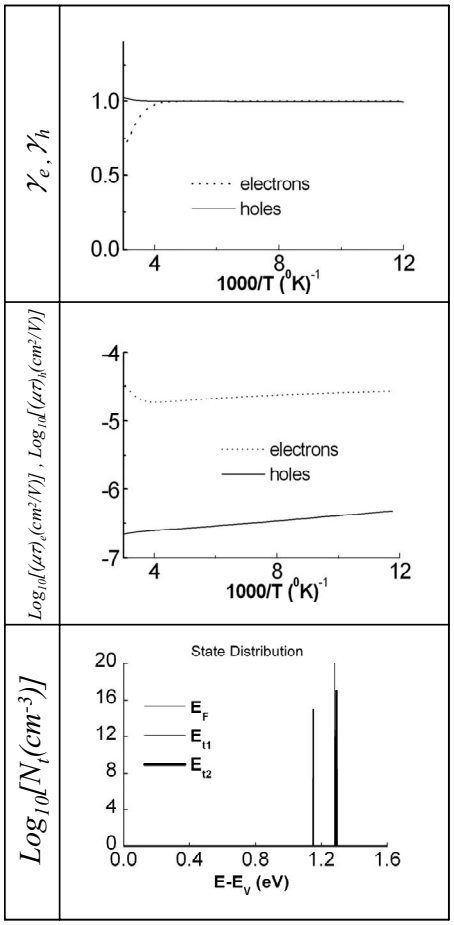

FIG. 5. The simulated temperature dependence of the four phototransport properties and the corresponding energy levels of the two defect centers in the system when $E_F - E_v = 1.28$ eV. The other parameters in the system are as given in Table I, except that $G = 10^{21}$ cm^{-3} s^{-1}, $E_{t2} - E_v = 1.35$ eV, $C_{n2} = C_{p2} = 10^{-9}$ cm^3 s^{-1}, $C_{n1} = 10^{-10}$ cm^3 s^{-1}, $C_{p1} = 10^{-8}$ cm^3 s^{-1}, $N_{t1} = 10^{15}$ cm^{-3}, $N_{t2} = 10^{17}$ cm^{-3}, and $\mu_e = 10^3(300/T)^{0.6}$ cm^2/V s.

E_F. For the two-center model we have seen that we can reproduce the experimentally observed results if the level of one set of centers lies above E_F and the level of the other set of centers lies below E_F. Hence, the salient conclusion from the above results is that in order to reproduce the experimental results we need a distribution of states such that there are some that lie above E_F and some that lie below E_F. The simplest scenario of this possibility is that of one type of centers such that while they have the same character they have an energy-level distribution around E_F. As a corresponding plausible scenario we considered then a Gaussian distribution of defect states around a given level, E_{tG}, that lies close to E_F. The existence of a state distribution is quite reasonable physically since it may well be that the origin of the defect states in In-doped CdTe is in the grain boundaries or the dopant complexes, and both of these constitute of somewhat disordered systems as is well known to be the case in polycrystalline or microcrystalline materials.[21] In the present case, if DX centers are considered, it is likely that such a distribution will result from the corresponding distribution of the lattice distortions. On the other hand, a Gaussian-type distribution may arise in such a scenario since one would expect on physical-statistical grounds that the concentration of particular distortions will decrease with the degree of distortion as is the case in other disordered systems.[40]

Following the above considerations we turned to the study of the case of the Gaussian state distribution: $N(E) = N_{tG}(1/\sqrt{2\pi}W)\exp[-(E-E_{tG})^2/2W^2]$, where E_{tG} is the center of the Gaussian and W is its width. Such a distribution was previously used in studies of phototransport properties of amorphous[41] and microcrystalline[21] silicon. As initial values we considered first a peak density, N_{tG}, of 10^{15} cm^{-3} eV^{-1}, a reasonable peak width of $W = 5 \times 10^{-2}$ eV, and a common capture coefficient for electrons and holes with a value of 10^{-8} cm^3 s^{-1}. As to be expected the most interesting case appears to be the one in which $E_{tG} = E_F$. This is since, as with the single-level case, the enforced asymmetry in the occupation of the states ($E_c - E_F < E_F - E_v$) provides a higher concentration of electrons than holes in the recombination centers. Hence, the material is a weak n-type photoconductor. This effect strengthens with the increase in temperature yielding the decrease in γ_e and the increase in $(\mu\tau)_e$ at intermediate temperatures. On the other hand γ_h behaves as a classical minority carrier[30] with $\gamma_h = 1$. At still higher temperatures the role of n_o becomes important and $\gamma_e \to 1$ while τ_e decreases. This behavior is seen in Fig. 6.

Turning to the comparison with the experimental results shown in Fig. 2 the clear advantage of the Gaussian case, in comparison with that of the single-level case, is that the change in temperature causes a significant change in the occupation of centers *both above and below* E_F. The results in Fig. 6 (where we assumed a temperature independent μ_e) do indeed resemble the experimental results as far as the exponents are concerned but they do not show the expected decrease with temperature in either $(\mu\tau)_e$ or $(\mu\tau)_h$. Similarly, the fact that we did not see a temperature dependence in $(\mu\tau)_h$ for the Gaussian cases with $E_{tG} \ll E_F$ suggests that only the case with $E_{tG} > E_F$ may account for the experimental data. Translating that conclusion to the present model we have put E_{tG} above E_F. This is also expected to yield that the increase in temperature will excite electrons to a higher density of state regions which is "deeper" for the holes, and thus will cause the decrease in $(\mu\tau)_h$. In other words the concentration of hole-effective recombination sites will increase with temperature, thus yielding the decrease in $(\mu\tau)_h$. Indeed these expectations were fulfilled in our simulations. However, following the effect of the variation in the parameters, $E_{tG} - E_F$, N_{tG}, C_n, C_p, and G, within their reasonable limits (that can be gathered from the above discussions), did not yield a considerable decrease in γ_e around 200 K and the minimum of γ_e was always at temperatures higher than 300 K. The only change in the system parameters that got us very close to the experimental behavior was the shift of E_F deeper into the band gap, making the model corresponds to an even "weaker" n-type photoconductor. Indeed for $E_{tG} - E_F = 0.06$ eV and $E_F - E_v = 1.1$ eV the results resembled very much the experimental results of Fig. 2. These results were much the same for $E_F - E_v = 1.08 \pm 0.02$ eV. On the other hand, for $E_F - E_v = 1.00$ eV, we got a "temperature delayed"

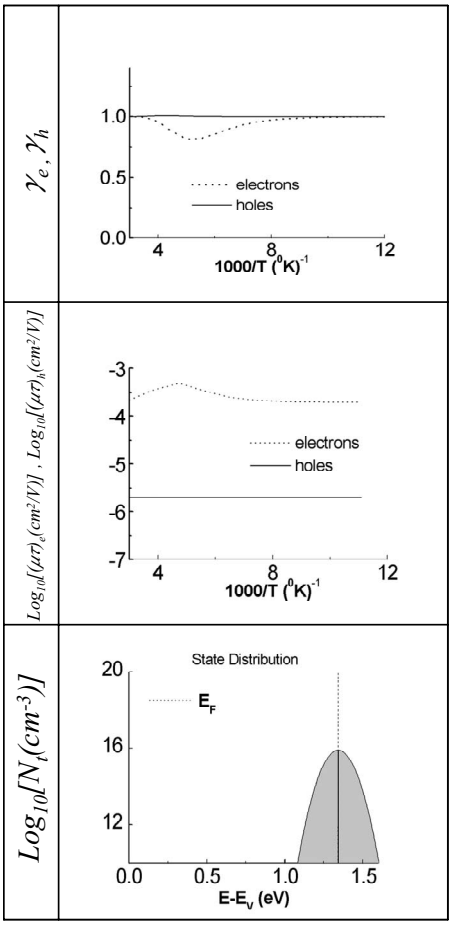

FIG. 6. The simulated temperature dependence of the four phototransport properties and the corresponding Gaussian defect-state distribution in the system. The parameters are as given in Table I but $E_{tG}-E_v=E_F-E_v=1.34$ eV.

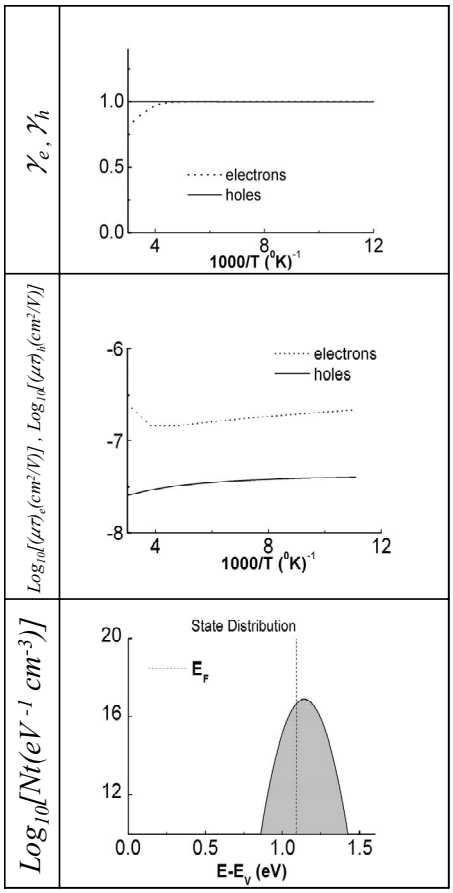

FIG. 7. The simulated temperature dependence of the four phototransport properties and the corresponding Gaussian defect-state distribution in the system. The parameters are as given in Table I but $E_F-E_v=1.08$ eV, $E_{tG}-E_v=1.14$ eV, $N_{tG}=10^{16}$ cm^{-3} eV^{-1}, $\mu_e=10(300/T)^{1/2}$ cm^2/V s, and $\mu_h=0.5$ cm^2/V s.

decrease in γ_e and, for $E_F-E_v=1.14$ eV, we got an exaggerated early decrease in γ_e. These provided then the limits to the E_F-E_v interval. The less significant role of the other parameters further emphasized that in addition to the $E_{tG}-E_F$ separation the energy interval E_F-E_v here is the other crucial parameter in the determination of the phototransport in the system, and that for this parameter the parameter space is very narrow. For example, the optimized value of W was found to be $W=0.05\pm0.01$ eV. Turning to the character of the states we found that the states can be neutral or acceptorlike, as long as the capture coefficients stayed around the 10^{-8} cm^3 s^{-1} value. Of course, pronounced donorlike states will "tip the balance" toward a more *p*-type photoconductor, as would a pronounced $E_{tG}<E_F$ scenario. This will yield however a disagreement with the experimental results.

Finally, our "fine tuned" model that includes the temperature dependence of μ_e is shown in Fig. 7. In order to have a quantitative fit we took now $\mu_e=10(300/T)^{1/2}$ cm^2/V s and $\mu_h=0.5$ cm^2/V s. We found of course very similar results when we interplayed between the values of the mobility and the values of the capture coefficients. Also, by very fine tuning we got the same results when we assumed mobilities of $\mu_e=300(300/T)^{1/2}$ cm^2/V s and $\mu_h=2$ cm^2/V s but with $E_{tG}-E_v=0.96$ eV and $C_n=C_p=10^{-7}$ cm^3 s^{-1}. The latter two changes are well understood since the shift of the γ_e minimum due to the increase in the capture coefficients will be compensated by the weaker *n*-type character that is achieved by taking E_F to be deeper while keeping the interval $E_{tG}-E_F$ constant. We see then that the $0.44\leq E_c-E_{tG}\leq0.49$ eV range that is used here is *consistent* with the E_F values that we estimated from our XPS and the dark conductivity results, when we assumed that E_F lies within a continuous distribution of states. These E_c-E_{tG} values are also in agreement with the values estimated in the literature.[42] We conclude then that the latter scenario provides a full and self-consistent account for the experimental results shown in Fig. 2.

VI. SUMMARY AND DISCUSSION

In this work we have studied the defect-state distribution and the recombination mechanism in In-doped CdTe films which is a system of a very wide interest. The determination of this distribution was enabled here by applying a step-by-step simulation method that is appropriate for bipolar semiconductors. In general, our method is based on the simple idea that the larger the number of available data sets the less

the number of arbitrary parameters that have to be assumed in the interpretation of the experimental results. This method, unlike the more common methods, gives the defect distribution throughout the entire band gap rather than in a limited portion of it. Also, in contrast with spectroscopic methods, the present method provides not only the energy levels of the defects but also their concentration and character. The most important aspect of the suggested method is however that it has stringent systematic self-consistency tests that are missing in the individual spectroscopic methods that were used thus far for the above purpose. On the other hand, our method, being based on macroscopic measurements, gives only the simplest (effective) possible scenario that can account for the observations rather than the detailed actual complicated scenario that may exist in the investigated material.

To appreciate the unavoidable necessity to apply methods such as ours for the derivation of the defect-state distribution maps from phototransport data we note that although the generalized Shockley-Read equations have an analytical solution for the simplest cases of the density of states (single or two discrete levels) the solutions are incredibly long (e.g., for the deep single-level case with negligible thermal emission the solutions of the three parameters n, p, and n_t take a third of an A4 page each). In fact, one cannot use those solutions in a legible way to follow the physical behavior of the system. This is, in particular, so if one wants to follow the dependence of the phototransport properties on an internal (such as capture coefficient) or an external (such as the temperature) parameter. Hence, a conspicuous advantage of our method is the direct numerical solution and the graphing of the four phototransport dependencies simultaneously. In addition, any other temperature-dependent quantity in the system could also be graphed (e.g., the charge-carrier concentrations in the different energy states and the recombination rate at each of them) so that the understanding of the recombination processes is made easier.

As we argue below, the comparison of our results with other data obtained on In-doped CdTe appears to show that indeed the method we presented can lead to quite a reliable and quantitative picture of the energy levels and the character distribution of the defects. In turn, this comparison will justify our presupposition that In-doped CdTe is a convenient vehicle for the demonstration of the usefulness of our method for the understanding of the basic physics of recombination. For example, a very satisfying outcome of this study is that the basic physics of recombination and photoconduction, as suggested originally by Rose,[28] is demonstrated. This is by showing the critical role of the position of E_F with respect to the defect-state distribution. We also provided an extension of the basic ideas of Rose[28] by giving quantitative limits to the corresponding position and by introducing the concept of the "center of gravity" of the states distribution. In addition, we were able to account for the behavior of both, the electrons and holes, as well as for the sharpness of the variations in the phototransport properties, not only due to the energetic position of the corresponding levels relative to E_F but also due to the effect of the other parameters in the system.

Another satisfying outcome of the present work is the ability to explain the data of Ref. 17 without resorting to the "mysterious" disappearance of defects with changing temperature. In that work, on Sn-doped CdTe, two main features in the density of states were found, one at $E_c-0.15$ eV and one at $E_c-0.36$ eV. As described in that work "the amplitude of the $E_c-0.36$ eV peak (but not the $E_c-0.15$ eV peak) appears to be strongly temperature dependent. The reason for this is presently unclear." To understand such a behavior one must realize that while the defect level structure does not change with temperature the photoelectronic "tools" that are used for the determination of this structure (as in this study and in Ref. 17) are sensitive to the conditions of the measurement (e.g., T and G). What one actually measures is the outcome of a convolution of the system's recombination properties and the sensitivity of the experimental tool. For example, in our analysis we saw that in the two-level scenario there is a competition between the recombination processes of the two levels, when one level lies above and one level lies below E_F. The result of this competition is determined of course by the various internal parameters of the system (such as C_n and C_p and the position of these levels) as well as by the opposing effects of the increase in G vs the increase in T. We have shown that for a given G the effect of increasing T is to shift the dominant recombination channel from the one above E_F to the one below E_F, and that the energy range where this happens (as emphasized by the variation in γ_e with T) is determined by the system parameters, in particular, the energetic separation of the two levels from E_F. Correspondingly, above a certain temperature, the lower level will become the dominant recombination channel. While the conditions that lead to the described behavior are specific, the fundamental physics follows the simple idea of Rose[28] that the increase in temperature provides enough hole-occupied recombination centers at the deeper level so that the main factor in determining the electrons lifetime is the recombination via that level.

Turning to our specific conclusions regarding the In-doped CdTe system let us examine our conclusion as given in Fig. 7 in light of the available data on such materials. Since comparing our results with the many data in the literature will lead to quite a long discussion (that deserves a review in its own right) and since a very recent work[42] on the subject, that can be considered to provide the state-of-the-art understanding of the system, is available, we have chosen to concentrate on a comparison of our results with the picture that emerges from that study. This will enable us to establish the validity of our method and discuss its limitations.

Babentsov *et al.*[42] have studied In-doped CdTe crystals with In contents in the $5\times10^{16}-7\times10^{17}$ cm^{-3} range while our polycrystalline films contained $\sim10^{18}$ cm^{-3} In atoms. They used however very different experimental methods to determine some of the defect parameters. Still, in the two studies it was found that the above concentrations were enough to render the material n type, and in both systems it was shown explicitly that E_F lies indeed above the midgap. The concluded $(\mu\tau)_e$ products in Ref. 42 were "lower than 10^{-5} cm^2/V" while we found few times 10^{-7} cm^2/V for $(\mu\tau)_e$ and few times 10^{-8} cm^2/V for $(\mu\tau)_h$. These differences in the $(\mu\tau)_e$ values are not unexpected in view of the possible different mobilities and defect concentrations in single crystals[42] and in polycrystalline films. Three electron

trapping levels were detected in the various spectra mentioned in Ref. 42, the deepest one at $E_c-0.65$ eV and the shallowest one at $E_c-0.25$ eV. Our results should be considered then as in "excellent agreement" with those findings following the fact that we found independently (see Fig. 7) that the center of gravity of the state distribution is around $E_c-0.46$ eV and that the Gaussian width of the distribution is 0.05 eV (so that defects at $E_c-0.56<E<E_c-0.2$ eV are detectable). For their above two corresponding electron trap levels they suggest, respectively, capture cross sections between 10^{-11} cm^2 and 3×10^{-15} cm^2 but no values of the hole capture cross sections were estimated there for the same defect states. In comparison, in our simulations we have concluded (see Fig. 7) that the cross sections (C_n/v_{th} and C_p/v_{th}, where v_{th} is the thermal velocity) for both, the electrons and the holes are on the order of 10^{-14} cm^2. Considering the differences between the two materials we conclude from the above comparison that there is at least a semiquantitative agreement between our results and the available state-of-the-art knowledge of the defect distribution in In-doped CdTe. Moreover, since our results present the simplest scenario that can account for the data one cannot expect this scenario to reproduce very specific details (such as how many different discrete energy levels are present in the system) as revealed by spectroscopic studies, but its application can give the most concise and thus effective model for the physical and practical evaluation of the system.

In our work we were not concerned with the microscopic origin of the defects as our method can only suggest the type of the defect states (neutral, donorlike or acceptorlike) but not their chemical and/or structural nature. On the other hand, the latter type characterization can help in speculations or confirmation of suggestions that follow atomic or chemical composition spectroscopies. This is of course common to all photoelectronic methods. Following that and the close resemblance described above with other data regarding the properties of the defects we can then speculate as to origin of the recombination centers that are detected in the present work as follows. The neutral-to-donor character of the centers of the higher levels, the large difference between the concentration of In atoms and the concentration of the free electrons in our material (see Sec. II) and the observation that in other (e.g., Sn-doped) CdTe *n*-type materials the levels were found at other energies than in In-doped CdTe, may suggest that In complexes are responsible for the defects detected here and in Ref. 42. This is consistent with conclusions derived by others. In addition then, the role of the In doping is to provide the shallow donors that elevate the Fermi level, E_F, that makes the material *n* type. Hence, further spectroscopic work will be needed in order to determine the chemical nature of the defect states in more detail.

In conclusion; in this work we have presented a self-consistent systematic method that can yield the simplest model for the defect distribution and the recombination mechanism in photoconductors. Using In-doped CdTe as a convenient test case we were able to show that the present method yields a reliable effective model for the description of this system as well as to demonstrate and extend the basic understanding of the role of the Fermi level position on the phototransport properties in bipolar semiconductors. In particular, we were able to show how this position determines the temperature dependencies of the phototransport properties of both the majority and minority carriers. In addition, we were able to resolve some puzzles concerning the *n*-type CdTe system and to derive a more quantitative understanding of the basic well-known models of Rose.

ACKNOWLEDGMENTS

This work was supported by the German Ministry for the Environment, Nature Conservation and Nuclear Safety under Project No. 032755U. The authors would like to thank Y. Goldstein for his valuable contribution to the work reported here. I.B. acknowledges the support of the Enrique Berman chair in Solar Energy Research at the HU.

APPENDIX A: THE BASIC RECOMBINATION MODEL AND ITS EQUATIONS

The generalization of the Schockley-Read[27] recombination model to more than one set of single-level centers is well known.[29] However, for the convenience of the reader we outline briefly the latter model along the lines that we presented previously for the two level system.[23] We also include the special case of a continuous distribution of states, as we applied in our previous works[21] but this time it is for a Gaussian distribution of states around a given center in the band gap.

Consider a system of m types of centers of which the energy levels E_i are given within the band gap E_c-E_v, where E_c and E_v are the conduction- and valence-band edges. These band edges have corresponding effective densities of states N_c and N_v. The concentration of each type of centers is N_i and they are characterized by their capture coefficients, C_{ni} for the electrons, and C_{pi} for the holes. Under a given temperature T and a carrier generation rate G there are steady-state concentrations of n electrons and p holes. Of these $n-n_o$ are photoexcited electrons and $p-p_o$ are photoexcited holes while n_o and p_o are the free carrier concentrations in the dark. Correspondingly, under illumination, the concentration of electron occupied centers of type i is n_{ti} and under dark it is n_{tio}. The generation-recombination processes (at E_c, E_v, and each E_i) can be presented by $m+1$ independent equations. In the steady state we have, at E_c, the generation of G electrons due to the light induced excitation from E_v as well as the thermal excitation from the centers, Σg_{ci}. These are balanced by the sum of the recombination rates at the centers, Σr_{ci}. The corresponding steady-state equation is then

$$G+\Sigma g_{ci}-\Sigma r_{ci}=0. \tag{A1}$$

Similarity, at each energy level i the balance of thermal generation and the recombination yields that

$$r_{ci}-r_{vi}+g_{vi}-g_{ci}=0, \tag{A2}$$

where r_{vi} is the rate of the recombination and g_{vi} is the thermal generation of the holes. The other equation that controls the kinetics is that of the charge neutrality that can be written as

$$n - n_o - p + p_o + \Sigma n_{ti} - \Sigma n_{tio} = 0, \tag{A3}$$

where $n_o = N_c f(E_c - E_F)$, $p_o = N_v[1 - f(E_c - E_F)]$, $n_{tio} = N_i f(E_i - E_F)$, and $f(E_c - E_F) = 1/\{1 + \exp[(E_c - E_F)/kT]\}$. We have then $m+2$ independent equations with the $m+2$ unknowns, n, p, and n_{ti}.

In the above equations,

$$g_{ci} = n_{ti} e_{ni}, \quad \text{where} \quad e_{ni} = C_{ni} N_c \exp[-(E_c - E_i)/kT], \tag{A4}$$

$$r_{ci} = C_{ni} n (N_i - n_{ti}), \tag{A5}$$

$$g_{vi} = (N_i - n_{ti}) e_{pi}, \quad \text{where} \quad e_{pi} = C_{pi} N_v \exp[-(E_i - E_v/kT], \tag{A6}$$

and

$$r_{vi} = C_{pi} p n_{ti}. \tag{A7}$$

In the present work, as in many previous works of others[29,41] and ours[21] we solved Eqs. (A1)–(A3) by the Newton-Raphson method[43] in order to find the above unknowns. We expressed then the mobility-lifetime products by

$$(\mu\tau)_e = (n - n_o)/G \quad \text{and} \quad (\mu\tau)_h = (p - p_o)/G, \tag{A8}$$

and we derived the light intensity exponents by the simple differentiation of these products, i.e.,

$$\gamma_e - 1 = d[\log_{10}(\mu\tau)_e]/d[\log_{10} G] \tag{A9}$$

and

$$\gamma_h - 1 = d[\log_{10}(\mu\tau)_h]/d[\log_{10} G]. \tag{A10}$$

Turning to the generalization of the above model to a set of centers that constitute of a continuous distribution of states we applied the detailed balance at a given energy level E. From Eq. (A2)d we have that the occupation probability f_t of a level at the energy E is given by

$$f_t(E) = n_t(E)/N_t(E) = (C_n n + C_p p)/[C_n(n + n_s) + C_p(p + p_s)], \tag{A11}$$

where $n_t(E)$ is the concentration of the electron occupied states at E, $N_t(E)$ is the total concentration of such states, $n_s = N_c \exp[-(E_c - E)/kT]$ and $p_s = N_v \exp[-(E - E_v)/kT]$. The total concentration of electrons in the occupied states in the above distribution is given by

$$n_t = \int N_t(E) f_t(E) dE, \tag{A12}$$

where the integration is over the entire band gap $E_c - E_v$. Under equilibrium $f_t(E)$ is simply the Fermi-Dirac function $f_{to}(E)$ and we have then that

$$n_{to} = \int N_t(E) f_{to}(E) dE. \tag{A13}$$

The effective contribution of this type of states to the charge neutrality Eq. (A3) is then $n_t - n_{to}$. The corresponding net recombination rate through this distribution $r_c - g_c$ is derived then from Eq. (A2) by noting that the concentration of holes at E is $N_t(E) - n_t(E)$ yielding that

$$r_c - g_c = \int \{N_t(E)[C_n C_p (np - n_o p_o)]/[C_n(n + n_s) + C_p(p + p_s)]\} dE. \tag{A14}$$

The latter equation replaces then the corresponding discrete level quantities in Eqs. (A1) and (A2). In the numerical calculation of the integrals [Eqs. (A12)–(A14)] we have applied the Simpson's rule method for numerical integration.

APPENDIX B: THE NUMERICAL SIMULATION

The simulation program that solves the set of Eqs. (A1)–(A3) was written in the "Microsoft Visual Basic 6.0 language pack." This language pack was preferred over others due to its convenient interface and reasonably high rate of operation.

The basic structure of the program was to solve a set of two independent equations taken out of the combination of Eqs. (A1)–(A3). Then, following the Newton-Raphson procedure of Ref. 43 we built a function that calculates the Jacobian of the two equations and calculates the next increment that the variables n and p must take in order to advance toward the solutions. This is until the convergence conditions are met. This function also iterates and tests the possibility of the convergence to a solution.

In order to calculate the increments of n and p the main process of the program uses six external functions for the two independent equations and their derivatives by n and p which are required for the calculation of the Jacobian. In the case of the continuous states distribution these six functions use an external function which integrates the distribution of states across the gap using Simpson's rule.

After one extracts the values of the n,p pair, it is straightforward to calculate the mobility lifetime product. For the light intensity exponents (defined in Sec. II) a calculation of a derivative is required. A "least-squares" method was employed then for several G values (usually $0.5G$, G, and $5G$) in order to extract the corresponding slope.

[1] B. Ray, *II-VI Compounds* (Pergamon Press, Oxford, 1969).

[2] K. Zanio, *Cadmium Telluride*, Semiconductors and Semimetals Vol. 13 (Academic, New York, 1978).

[3] For a detailed review of the properties of CdTe and its relevance to solar cells, see, R. H. Bube, *Photovoltaic Materials* (Imperial College, Singapore, 1998); for a recent work on this subject see O. Vigil-Galan, E. Sanchez-Meza, C. M. Ruiz, J. Sastre-Hernandez, A. Morales-Acevedo, F. Cruz-Gandarillo, E. Suceda, G. Contrerasas-Puente, and V. Bermudez, Thin Solid Films **515**, 5819 (2007), and references therein.

[4] For a general review see D. Redfield and R. H. Bube, *Photoinduced Defects in Semiconductors* (Cambridge University Press, Cambridge, 1996).

[5] F. J. Espinosa, J. M. de Leon, S. D. Conradson, J. L. Pena, M. Zapata-Torres, and P. E. Wolf, Phys. Rev. Lett. **83**, 3446 (1999), and references therein.

[6] R. Castro-Rodriquez and J. L. Pena, J. Vac. Sci. Technol. A **11**, 730 (1993).

[7] Z. Rivera-Alvarez, L. Hernández, M. Becerril, A. Picos-Vega, O. Zelaya-Angel, R. Ramı´rez-Bon, and J. R. Vargas-Garcı´a, Solid State Commun. **113**, 621 (2000).

[8] R. A. Linke, T. Thio, J. D. Chadi, and G. E. Devlin, Appl. Phys. Lett. **65**, 16 (1994).

[9] C. Longeaud, J. P. Kleider, and M. Cuniot, Opt. Mater. **4**, 271 (1995).

[10] Y. Eisen, Nucl. Instrum. Methods Phys. Res. A **322**, 596 (1992); R. H. Redus, A. C. Huber, and J. A. Pantazis, *ibid.* **458**, 214 (2001).

[11] P. von Huth, J. E. Butler, W. Jaegermann, and R. Tenne, J. Electrochem. Soc., **149**, G55 (2002); P. von Huth, J. E. Butler, and R. Tenne, Sol. Energy Mater. Sol. Cells **69**, 381 (2001).

[12] D. J. Chadi, Phys. Rev. Lett. **72**, 534 (1994); **79**, 4834 (1997).

[13] S. W. Biernacki, Solid State Commun. **88**, 365 (1993).

[14] C. H. Park and D. J. Chadi, Appl. Phys. Lett. **66**, 3167 (1995); Phys. Rev. B **52**, 11884 (1995), and references therein.

[15] O. Panchuk, A. Savitskiy, F. Fochuk, Ye. Nykonyuk, O. Parfenyuk, L. Shcherbak, M. Ilashchuk, L. Yatsunyk, and P. Feychuk, J. Cryst. Growth **197**, 607 (1999).

[16] E. Saucedo, C. M. Ruiz, V. Bermudez, E. Dieduez, E. Gombia, A. Zappettini, A. Baraldi, and N. V. Sochinski, J. Appl. Phys. **100**, 104901 (2006).

[17] M. J. Gueorguieva, C. Main, S. Reynolds, R. Brüggemann, and C. Longeaud, J. Non-Cryst. Solids **299-302**, 541 (2002).

[18] S. R. Das, J. G. Cook, and G. Mukhherjee, J. Appl. Phys. **69**, 8210 (1991).

[19] For a detailed compilation of data see X. Mathew, Sol. Energy Mater. Sol. Cells **76**, 225 (2003).

[20] C.-P. Ye and J. H. Chen, J. Appl. Phys. **67**, 2475 (1990).

[21] I. Balberg, Y. Dover, R. Naides, J. P. Conde, and V. Chu, Phys. Rev. B **69**, 035203 (2004).

[22] I. Balberg, J. Non-Cryst. Solids **299-302**, 531 (2002).

[23] Y. Lubianiker, G. Biton, I. Balberg, T. Walter, H. W. Schock, O. Resto, and S. Z. Weisz, J. Appl. Phys. **79**, 876 (1996).

[24] I. Balberg, R. Naidis, M.-K. Lee, J. Shinar, and L. F. Fonseca, Appl. Phys. Lett. **79**, 197 (2001).

[25] I. Balberg and R. Naidis, Phys. Rev. B **57**, R6783 (1998); I. Balberg and Y. Lubianiker, *ibid.* **48**, 8709 (1993), and references therein.

[26] For an introduction see J. W. Orton and P. Blood, *The Electrical Characterization of Semiconductors: Measurement of Minority Carrier Properties*, (Academic Press, London, 1990); and for a review, see I. Balberg, *Amorphous Silicon Technology*, MRS Symposia Proceedings No. 258 (Materials Research Society, Pittsburgh, 1992), p. 693.

[27] H. Shockley and W. T. Read, Jr., Phys. Rev. **87**, 835 (1952).

[28] A. Rose, *Concepts in Photoconductivity and Allied Problems* (Interscience, New York, 1963).

[29] R. H. Bube, *Photoelectronic Properties of Semiconductors* (Cambridge University, Cambridge, 1992).

[30] I. Balberg, J. Appl. Phys. **75**, 914 (1994).

[31] S. M. Sze and K. K. Ng, *Physics of Semiconductor Devices* (Wiley, Hoboken, 2007).

[32] Y. Lubianiker and I. Balberg, Phys. Rev. Lett. **78**, 2433 (1997).

[33] N. F. Mott and E. A. Davis, *Electronic Processes in Non-Crystalline Materials* (Clarendon Press, Oxford, 1971).

[34] H. Overhof and P. Thomas, *Electronic Transport in Hydrogenated Amorphous Semiconductors* (Springer-Verlag, Berlin, 1989).

[35] A. A. El-Mongy, A. A. Belal, H. El Sheikh, and A. El Amin, J. Phys. D **30**, 161 (1997).

[36] J. Franc, R. Grill, L. Turjanska, P. Hoschl, E. Belas, and P. Moravec, J. Appl. Phys. **89**, 786 (2001).

[37] X. Yang, C. Xu, and N. C. Giles, J. Appl. Phys. **104**, 073727 (2008).

[38] J. Moesslein, A. Lopes-Otero, A. L. Fahbebruch, D. Kim, and R. H. Bube, J. Appl. Phys. **73**, 8359 (1993).

[39] P. T. Landsberg, *Recombination in Semiconductors* (Cambridge University Press, Cambridge, 1991).

[40] S. K. O'Leary and P. K. Lim, Solid State Commun. **101**, 513 (1997).

[41] M. Q. Tran, Philos. Mag. B **72**, 35 (1995).

[42] V. Babentsov, J. Franc, and R. B. James, Appl. Phys. Lett. **94**, 052102 (2009), and references therein.

[43] W. H. Press, B. P. Flannery, S. A. Teukalstay, and W. A. Vetterling, *Numerical Recipes* (Cambridge University Press, London, 1986), Chap. 9.